Soliton density in Rb_2ZnBr_4

R. Blinc, V. Rutar, B. Topič, F. Milia,* and Th. Rasing†
J. Stefan Institute, E. Kardelj University of Ljubljana, Ljubljana, Yugoslavia
(Received 28 May 1985)

The modulation wave in Rb_2ZnBr_4 is pinned over most of the incommensurate phase and ^{87}Rb NMR line-shape analysis cannot distinguish between a true incommensurate phase and a large-period commensurate phase with $N=17$. The temperature variations of the soliton density, the line shape, and the spin-lattice relaxation rate speak for the coexistence of a large number of domains pinned by impurities rather than for the existence of a devil's staircase and pinning by the discreteness of the crystal lattice. The large thermal hysteresis in the soliton density demonstrates the presence of a metastable, impurity-induced "chaotic" phase with random intersoliton spacing which exists even far below the incommensurate-commensurate transition.

I. INTRODUCTION

Rb_2ZnBr_4 represents one of the first known examples of one dimensionally modulated incommensurate insulators.[1–10] The nature of the incommensurate phase in Rb_2ZnBr_4 between $T_I=346$ K and $T_c=187$ K, however, is still far from being well understood. In contrast to isomorphous Rb_2ZnCl_4 and K_2ZnCl_4 and in contrast to the predictions of the Landau theory,[11] the modulation wave vector does not change with temperature over more than 140 K. It has been recently found[5,6] that in the high-temperature part of the incommensurate phase the modulation wave vector equals $\frac{5}{17}$ so the unit cell should be in fact commensurate and 17 times larger than in the high-temperature phase above T_I. This result is rather unusual since commensurate phases with a large superstructure should exist over a narrower range of temperatures than phases with a small superstructure. Another suprising result is that close to the incommensurate-commensurate transition successive jumps in the modulation wave vector were observed, but the various "steps" are not specified by an exact fraction as predicted in the devil's-staircase model[7] and, moreover, seem to coexist in a certain temperature range.[5,6]

Experimentally, it is rather hard to distinguish higher-order commensurate phases with large periods from true incommensurate phases.[8,9] Here we wish to investigate what ^{87}Rb $\frac{1}{2}\rightarrow-\frac{1}{2}$ quadrupole perturbed nuclear magnetic resonance can say about the nature of the incommensurate phase in Rb_2ZnBr_4. We wish as well to redetermine[10] the soliton density in this system using recently improved line-shape analysis techniques.

II. LANDAU THEORY

A. The soliton density and the Landau theory

For systems of interest like Rb_2ZnBr_4, $(NH_4)_2BeF_4$, etc., where the order parameter Q has two components, the Landau free-energy density can be expressed[11] as

$$g(x)=\frac{\alpha}{2}(Q^*Q)+\frac{\beta}{4}(Q^*Q)^2-\frac{\gamma}{2}[Q^n+(Q^*)^n-(Q^*Q)^{n/2}]$$
$$-i\frac{\delta}{2}\left[Q\frac{dQ^*}{dx}-Q^*\frac{dQ}{dx}\right]+\frac{\kappa}{2}\left|\frac{dQ}{dx}\right|^2 . \quad (1)$$

Here Q is complex. For convenience we have retained a higher-order term $(Q^*Q)^{n/2}$ considering only even n, e.g., $n=10$ for $[N(CH_3)_4]_2ZnCl_4$, $n=6$ for Rb_2ZnCl_4, $n=4$ for $(NH_4)_2BeF_4$, and $n=2$ for chiral smectic liquid crystals in an external magnetic field. Here we have $\alpha=\alpha_0(T-T_0)$ and $\beta,\kappa,\gamma,\delta>0$. Introducing polar coordinates $Q=A\exp(i\varphi)$, Eq. (1) can be rewritten as

$$g(x)=\frac{\alpha}{2}A^2+\frac{\beta}{4}A^4+\gamma A^n\cos^2\left[\frac{n\varphi}{2}\right]$$
$$-\delta A^2\varphi'+\frac{\kappa}{2}A^2(\varphi')^2 . \quad (2)$$

Minimizing

$$F=\frac{1}{x_0}\int_0^{x_0}g(x)dx$$

with respect to φ in the constant-amplitude approximation $A=A_0\neq A(x)$ and making use of the identity

$$\cos^2(n\varphi/2)=[1+\cos(n\varphi)]/2 ,$$

one finds the Euler equation for our problem (i.e., the sine-Gordon equation)

$$\frac{\partial g}{\partial\varphi}-\frac{d}{dx}\frac{\partial g}{\partial\varphi'}=0 , \quad (3a)$$

yielding

$$\kappa\varphi''=-\frac{n}{2}\gamma A_0^{n-2}\sin(n\varphi) \quad (3b)$$

with $\varphi'=d\varphi/dx$ and $\varphi''=d^2\varphi/dx^2$.

The first integral of this equation is

$$\frac{\kappa}{2}(\varphi')^2=\eta+\frac{\gamma}{2}A_0^{n-2}[\cos(n\varphi)-1]$$
$$=\eta-\gamma A_0^{n-2}\sin^2\left[\frac{n}{2}\varphi\right], \tag{4}$$

where η is an integration constant. The maximum value of the derivative of the phase, $\varphi'_{\max}$, determines the soliton width d_0 (Fig. 1), which is given by

$$\varphi'_{\max}=\frac{2\pi}{d_0 n}=\left[\frac{2\eta}{\kappa}\right]^{1/2}. \tag{5}$$

The intersoliton distance is, on the other hand, obtained as

$$x_0=\left[\frac{\kappa}{2}\right]^{1/2}\int_0^{2\pi/n}\frac{d\varphi}{\left[\eta-\gamma A_0^{n-2}\sin^2\left[\frac{n}{2}\varphi\right]\right]^{1/2}}. \tag{6}$$

Introducing a new variable $\phi=(n/2)\varphi$, we can express x_0 as

$$x_0=\left[\frac{\kappa}{2\gamma A_0^{n-2}}\right]^{1/2}\frac{4}{n}kK(k), \tag{7}$$

where $K(k)$ is the complete elliptic integral of first kind,

$$K(k)=\int_0^{\pi/2}\frac{d\phi}{(1-k^2\sin^2\phi)^{1/2}}, \tag{8a}$$

and

$$k^2=\frac{1}{1+\Delta^2}=\frac{\gamma A_0^{n-2}}{\eta}. \tag{8b}$$

The relation between φ and x as well as between x_0 and d_0 is illustrated in Fig. 1 both for large and small Δ.

The soliton density which measures the volume fraction of the crystal in the incommensurate domain walls[12] is now obtained as

$$n_s=\frac{d_0}{x_0}=\frac{\pi/2}{K(k)}. \tag{9}$$

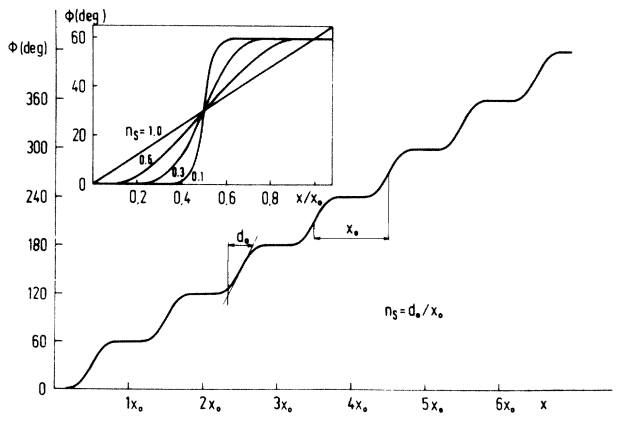

FIG. 1. Spatial variation of the phase φ of the modulation wave for different soliton densities $n_s=d_0/x_0$. Here d_0 is the soliton width and x_0 the intersoliton spacing. The spatial variable x is measured in units of x_0.

It should be noticed that the soliton density n_s as defined above measures the "domain-wall fraction" and it is not equal to the inverse soliton separation $1/x_0$ which measures the number of solitons per unit length. Since the soliton width d_0 only weakly depends on temperature, these two quantities are proportional to each other. On approaching the plane-wave limit the soliton separations are of the same order or smaller than the soliton width; therefore n_s as defined above gives a better description of the true physical situation than $1/x_0$. The parameter k is within the constant-amplitude approximation determined by minimizing

$$F=\frac{1}{x_0}\int_0^{x_0}g(x)dx$$

with respect to η, yielding

$$\frac{E(k)}{k}=\frac{\pi}{4}\delta\left[\frac{2}{\kappa\gamma A_0^{n-2}}\right]^{1/2}. \tag{10}$$

The temperature T enters the above expression through the amplitude of the order parameter, $A_0^2=\alpha_0(T_I-T)/\beta$. Here $E(k)$ is the complete elliptic integral of the second kind,

$$E(k)=\int_0^{\pi/2}(1-k^2\sin^2\phi)^{1/2}d\phi.$$

It should be noticed that for $T\to T_I$ (i.e., $A_0\to 0$), $k\to 0$, $\Delta^2\to\infty$, and $K(k)\to\pi/2$, so that $n_s\to 1$. For $T\to T_c$ one finds, on the other hand, $\Delta^2\to 0$, $k^2\to 1$, $K(k)\to\infty$, and $n_s\to 0$. It should be also pointed out that the soliton density n_s and the density of the commensurate domains, n_c, are related by $n_s+n_c=1$. The temperature dependences of n_c and n_s, as predicted by the Landau theory, are illustrated in Figs. 2 and 3. The constant-amplitude approximation $A=A_0=A(x)$ breaks down[13] very close to T_c.

It should be stressed that the temperature dependences of the soliton density n_s and the incommensurate wave vector $q=2\pi/x_0$ are qualitatively different both in the constant-amplitude approximation, $A=A_0$, and in the more realistic case with $A=A(x)$. The difference is due to the temperature dependence of the soliton width d_0. Near T_I, d_0 decreases with decreasing temperature faster than x_0, resulting in a rather smooth drop of n_s though $q=2\pi/x_0$ is nearly constant. Close to T_c, x_0 is critical and n_s and q vanish in the same way.

If the continuum approximation is dropped and the discreteness of the crystal structure is taken into account, a chaotic phase intermediate between the incommensurate and commensurate phases should occur.[14] The same is true if defects are taken into account.[15] Quenched random impurities destroy[15] the long-range order in the incommensurate phase below $d=4$ dimensions and lead to the formation of domains. Hence T_I and T_c mark no phase transitions in the strict sense if quenched disorder is taken into account.

B. The NMR line shape

The real displacement $\mathbf{u}$ of the ith nucleus in an incommensurate phase is an admixture of a symmetric and an

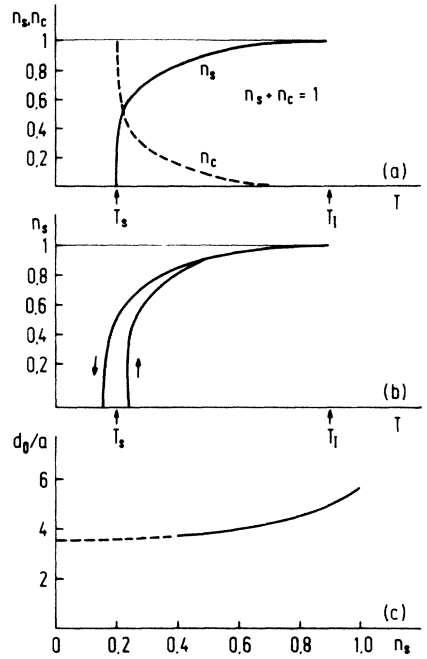

FIG. 2. (a) Temperature dependences of the soliton density n_s and the density of the commensurate domains n_c according to the Landau theory (——), (b) if pinning and nucleation is considered (. . . .), and (c) the T dependence of the soliton width d_0 according to the Landau theory.

antisymmetric component:

$$\mathbf{u}_i = \mathbf{u}_{0i}^c \cos[\phi(x_i)] + \mathbf{u}_{0i}^s \sin[\phi(x_i)] , \tag{11}$$

so that the components of the displacement vector u_{ik} ($k = x,y,z$) can be expressed as

$$u_{ik} = u_{oik} \cos[\phi(x_i) + \phi_{ik}^{(0)}], \quad k = x,y,z \tag{12}$$

where $\phi_{ik}^{(0)}$ is different for different nuclei in the unit cell. Here $\phi(x_i) = \mathbf{q}_c \cdot \mathbf{x}_i + \varphi(x)$ with $\mathbf{q}_c$ standing for the commensurate part of the modulation vector $[\mathbf{q}_I = \mathbf{q}_c(1-\delta)]$ and $\varphi(x)$ for a solution of the sine-Gordon equation. The position of the ith nucleus in the lth unit cell of the high-temperature phase is designated by

$$\mathbf{x}_i(l) = \mathbf{x}_{0i} + l\mathbf{a}, \quad l = 0,1,2,3 \ldots .$$

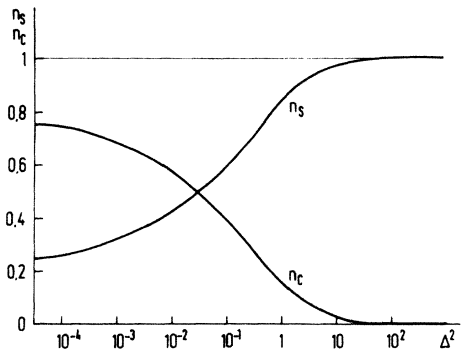

FIG. 3. Variation of n_s and n_c with Δ^2.

The expansion of the NMR frequency in powers of the nuclear displacements is no longer of the special local form[12] $\nu_i = \nu(u_i(x))$, but contains[16] both sine and cosine terms.

The same situation arises if the relation between the frequency and the nuclear displacements is nonlocal:[16]

$$\nu_i = \nu(u_i(x_i), u_j(x_j), \ldots) . \tag{13}$$

In both cases one finds[16]

$$\nu(x) = \nu_0 + \nu_{1c}\cos[\phi(x)] + \nu_{1s}\sin[\phi(x)] + \tfrac{1}{2}\nu_2' + \nu_{2c}\cos[2\phi(x)] + \nu_{2s}\sin[2\phi(x)] \cdots . \tag{14}$$

This can be rearranged as

$$\nu(x) = \nu_0 + \nu_1 \cos[\psi(x) + \tilde{\phi}_0] + \nu_2' + \nu_2 \cos^2[\psi(x)] + \cdots , \tag{15}$$

where $\psi(x)$ and $\tilde{\phi}_0$ are renormalized phases.[16]

The frequency distribution function for a static one-dimensionally modulated incommensurate system is, in the constant-amplitude approximation, obtained[12,16] as

$$f(\nu) = \frac{\text{const}}{d\nu/dx} + \frac{\text{const}}{(d\nu/d\psi)(d\psi/dx)} . \tag{16}$$

Singularities will appear in the spectrum when (i) $d\nu/d\psi \to 0$, and/or (ii) $d\psi/dx \to 0$.

In the plane-wave limit $d\psi/dx = \text{const}$ and the only singularities are associated with $d\nu/d\psi \to 0$. In the multisoliton lattice limit the phase ψ will be nearly constant in the "commensurate" domains where $d\psi/dx \to 0$, whereas it will vary with x in the "solitonlike" domain walls where $d\psi/dx \neq 0$. The appearance of "commensurate" domains will thus result in the appearance of new "commensurate" lines and in a reduction of the intensity of the incommensurate background and edge singularities.

Expressing $\psi(x) = \varphi(x) + \phi_0$, we can rewrite Eq. (4) as

$$\frac{d\psi}{dx} = \text{const} \times \{\Delta^2 + \cos^2[n(\psi - \phi_0)/2]\}^{1/2} , \tag{17}$$

where Δ^2 is related to the soliton density n_s by Eqs. (8b) and (9), with

$$K(k) = K\left[\frac{1}{(1+\Delta^2)^{1/2}}\right]$$

being defined by Eq. (8a). Here Δ^2 is determined from the experiment by fitting the observed line shape to Eqs. (16) and (17).

Expression (17) yields up to n new "commensurate" lines for $\Delta \to 0$ in addition to the incommensurate edge singularities arising from $d\nu/d\psi \to 0$. The new lines will appear for $\Delta \ll 1$ when $\cos^2[n(\psi - \phi_0)/2] = 0$, i.e., when

$$\psi = (2m+1)\pi/n + \phi_0, \quad m = 0,1,2, \ldots, n-1 . \tag{18}$$

In the commensurate phase $\psi(x)$ and $\varphi(x)$ become constants which just renormalize the phase shift $\phi_0 \to \tilde{\phi}_0$. Expressing the commensurate wave vector $\mathbf{q}_c$ characterizing a given commensurate phase as

$$\mathbf{q}_c = \mathbf{b}^* \frac{M}{N} , \tag{19}$$

where $\mathbf{b}^*$ is a reciprocal-lattice vector of the high-temperature phase and M,N are integers, relation (15) can be written in the simplest linear case ($\nu_2=\nu_2'=0$) as

$$\nu^{(M,N)}=\nu_0+\nu_1\cos\left[2\pi\frac{M}{N}+\tilde{\phi}_0\right],\quad M=0,1,2,\ldots,N-1\ . \tag{20}$$

Relation (20) yields the NMR frequencies in a commensurate cell which is N times larger than the high-temperature cell. The frequency distribution is now a sum of δ functions

$$f(\nu)=\frac{1}{N}\sum_{M=0}^{N-1}\delta(\nu-\nu^{M,N}) \tag{21}$$

yielding[17] N commensurate instead of the quasicontinuous incommensurate frequency distribution.[16] The splittings between these lines will vary with N roughly as[16] $\Delta\nu=2\nu_1/(N-1)$. The commensurate peaks will be smeared out and indistinguishable from an incommensurate plane-wave-type line shape if the natural linewidth of the individual lines is larger than $\Delta\nu$.

It should be noted that on going from one commensurate supercell to another in the devil's-staircase model, N will vary discontinuously whereas the amplitude A and ν_1 will be continuous. Still another quantity which will vary with N is the commensurability gap in the phase-fluctuation spectrum,[9]

$$\Delta_c^2=K^2N^2A^{N/2-2}\ . \tag{22}$$

Here KN is of the order of a phonon frequency and as $|A|\leq 1$, the phase-fluctuation gap Δ_c goes to zero as $N\rightarrow\infty$, i.e., as the truly incommensurate phase is approached.

III. RESULTS AND DISCUSSION

A. Incommensurate or higher-order commensurate phases

The ^{87}Rb $\frac{1}{2}\rightarrow-\frac{1}{2}$ NMR lines[4,10] in Rb_2ZnBr_4 are significantly broader than in Rb_2ZnCl_4 and the resolution is not good enough to discriminate[17] between a true incommensurate phase and a higher-order commensurate phase with $N=17$.

Except[18] very close to T_I, the modulation wave is static and pinned similarly as in other incommensurate systems. Several arguments which speak for pinning by impurities and against the possibility of a pinning due to the discreteness of the crystal lattice and the existence of a devil's staircase in Rb_2ZnBr_4 are the following.

(i) The floating[18] of the modulation wave close to T_I is similar to that in Rb_2ZnCl_4.[19]

(ii) The phase- and the amplitude-fluctuation branches in Rb_2ZnBr_4 have been clearly identified.[10] The phase gap in the incommensurate phase—as measured by the phase-fluctuation induced spin-lattice relaxation rate[4,10]—is of the same order as in Rb_2ZnCl_4, where it is defect induced.

(iii) In the low-temperature part of the incommensurate phase, "commensurate" peaks appear, indicating the transition from the plane wave to the multisoliton lattice-type modulation regime. If these peaks indicated transitions from one commensurate supercell to another, the changes would be less continuous than observed and would, moreover, be accompanied by jumps in the phase-fluctuation-induced T_1 as observed[20] in $[N(CH_3)_4]_2ZnCl_4$ but not in Rb_2ZnBr_4.

(iv) The incommensurate-commensurate transition in Rb_2ZnBr_4 is accompanied by a jump in the phase-fluctuation-induced T_1, which is of the same order as in Rb_2ZnCl_4.[17,20]

We thus believe that the modulation wave in Rb_2ZnBr_4 is pinned by defects and that the observed behavior[5,6] close to the incommensurate-commensurate transition is due to a large number of coexisting long-period phases or domains due to pinning by frozen impurities,[15] which destroy long-range order in the strict sense. The fact that in some samples the incommensurate-commensurate transition could not be observed at all supports this conclusion.

B. The soliton density and its T dependence

The temperature dependence of the line splitting is shown in Fig. 4 for $\mathbf{a}\perp\mathbf{H}_0, \measuredangle\, \mathbf{b},\mathbf{H}_0=162°$. The relation between the nuclear resonance frequency and the nuclear displacements is here such that the linear term is dominant. The splitting can be fitted by $\nu_1=35$ kHz and $\tilde{\phi}_0=0$. A comparison between the experimental and theoretical line shapes is given in Fig. 5 for Rb(2). The commensurate lines appearing at the center of the spectrum are clearly visible and gradually increase in intensity on approaching T_c, whereas the other two groups of commensurate lines merge with the edge singularities. The critical exponent β is 0.36 ± 0.04 and n_s has qualitatively—though not quantitatively—a similar behavior as in Rb_2ZnCl_4.[8,9] On cooling n_s is nonzero at T_c, demonstrating the existence of metastable randomly pinned solitons which persist even below T_c. The density of pinned solitons at T_c is considerably higher here than in Rb_2ZnCl_4.[8,9] This seems to be due to a greater concentration of impurities (i.e., Cl admixtures), thus suggesting that the metastable chaotic phase[14]—intermediate between the incommensurate and commensurate phases—is defect induced.

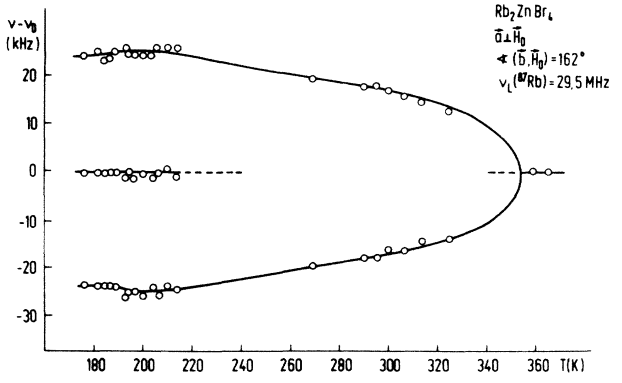

FIG. 4. Temperature dependence of the splitting of the ^{87}Rb $\frac{1}{2}\rightarrow-\frac{1}{2}$ spectra in Rb_2ZnBr_4 at an orientation where the linear term is dominant.

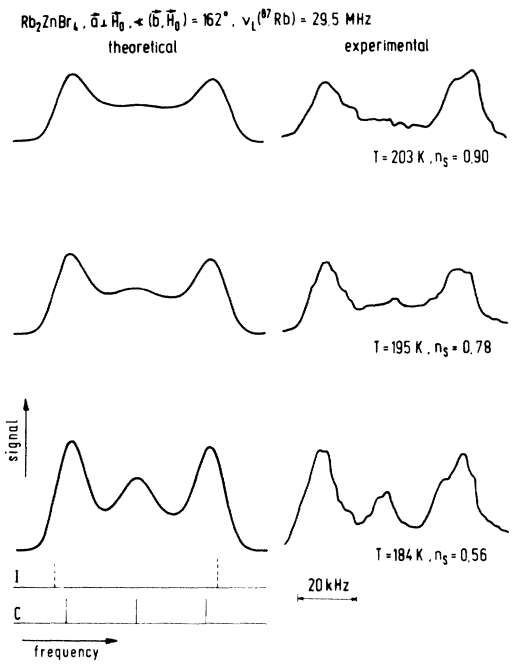

FIG. 5. Comparison between experimental and theoretical line shapes in Rb_2ZnBr_4 for the case that the linear term in expansion (15) is dominant. The coefficients are given in the text. The positions of the incommensurate (I) edge singularities at $(\nu-\nu_0)/\nu_1=-1$ are shown by dashed vertical lines, whereas the positions of the commensurate (C) lines at $(\nu-\nu_0)/\nu_1=0,\pm0.87$ are shown by solid lines at the bottom of the figure.

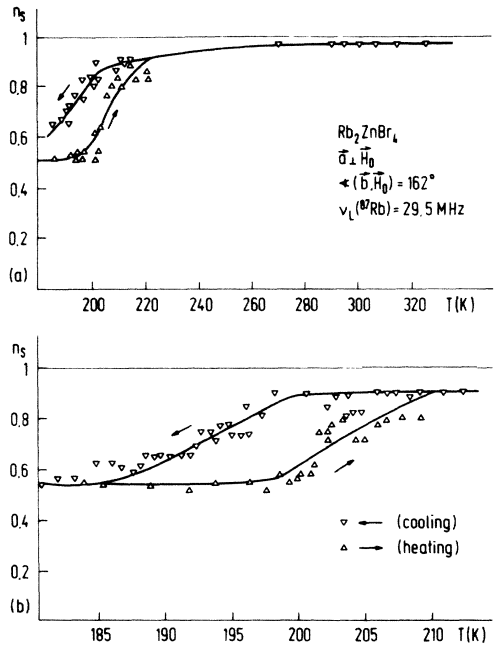

FIG. 6. Temperature dependence of the soliton density n_s in Rb_2ZnBr_4 obtained by a comparison of experimental and theoretical line shapes for $n=6$ in the constant-amplitude approximation.

The temperature dependence of the soliton density in Rb_2ZnBr_4 (Fig. 6) is qualitatively similar to the one in Rb_2ZnCl_4 but there are several important differences:

(i) The soliton density n_s in Rb_2ZnBr_4 is practically constant and equal to the plane-wave modulation value 0.97 ± 0.03 within a temperature interval of more than 100 K, i.e., from $T_I \approx +80$ to -40°C in sharp contrast to Rb_2ZnCl_4, where it continuously varies with temperature.

(ii) The ^{87}Rb $\frac{1}{2}\rightarrow-\frac{1}{2}$ NMR lines measured by the spin-echo techniques are much broader than in Rb_2ZnCl_4, thus showing the presence of impurities. In addition to the lines shown in Fig. 5, there is a broad background due to Rb nuclei in the vicinity of defects.

(iii) Close to T_c in the I phase, as well as below T_c in the commensurate phase, a large thermal hysteresis of 10—15 K (Fig. 6) is n_s is observed. On cooling the lowest observed value of n_s at T_c is 0.65, whereas the value of n_s at T_c on heating from low T is about 0.5. Here T_c is determined by the jump[10] in T_1. The n_s values are as well rather high if one cools the sample below T_c, demonstrating the presence of a metastable chaotic phase with randomly pinned solitons similar to the one observed[19] in Rb_2ZnCl_4.

The differences between the present n_s results and the results of Ref. 10 are mainly due to the fact that in Ref. 10 the soliton density was determined from the intensity of the commensurate lines and not from a line-shape analysis.

*On leave of absence from Nuclear Research Center "Demokritos" Aghia Paraskevi Attikis, Athens, Greece.

†Present address: Research Institute for Materials, University of Nijmegen, Toernooiveld, 6525 ED Nijmegen, The Netherlands.

[1]C. J. de Pater and C. van Dijk, Phys. Rev. B **18**, 1281 (1978).

[2]K. Gesi and M. Iizumi, J. Phys. Soc. Jpn. **45**, 1777 (1978).

[3]H. Jacobi, Z. Kristallogr. Kristallogeom. Kristalphys. Kristalchem. **135**, 467 (1972).

[4]R. Blinc, V. Rutar, J. Seliger, S. Žumer, Th. Rasing, and I. P. Aleksandrova, Solid State Commun. **34**, 895 (1980).

[5]A. C. R. Hogervorst and P. M. de Wolf, Solid State Commun. **43**, 179 (1982).

[6]M. Iizumi and K. Gesi, J. Phys. Soc. Jpn. **52**, 2526 (1983).

[7]S. Aubry, Ferroelectrics **24**, 53 (1980), and references therein.

[8]V. A. Golovko and A. P. Levanyuk, Fiz. Tverd. Tela (Leningrad) **23**, 3170 (1981) [Sov. Phys.—Solid State **23**, 1844 (1981)].

[9]V. A. Golovko and A. P. Levanyuk, Fiz. Tverd. Tela (Leningrad) **23**, 3179 (1981) [Sov. Phys.—Solid State **23**, 1850 (1981)].

[10]V. Rutar, F. Milia, B. Topič, R. Blinc, and Th. Rasing, Phys. Rev. B **25**, 281 (1982).

[11]P. Prelovšek, J. Phys. C **15**, L269 (1982).

[12]R. Blinc, Phys. Rep. **79**, 331 (1981), and references therein.

[13]R. Blinc, P. Prelovšek, and R. Kind, Phys. Rev. B **27**, 5404 (1983).

[14]P. Bak and V. L. Pokrovsky, Phys. Rev. Lett. **79**, 331 (1981).

[15]Y. Imry and S. Ma, Phys. Rev. Lett. **35**, 1399 (1975).
[16]R. Blinc, in *Proceedings of the XXIInd Congress Ampere,* edited by K. A. Müller, R. Kind, and J. Roos, The University of Zürich, Zürich, 1984), p. 23; R. Blinc, J. Seliger, and S. Žumer, J. Phys. C **18**, 2313 (1985).
[17]R. Blinc, S. Žumer, D. C. Ailion, and J. Nicponski, J. Phys. (Paris) **46**, 1205 (1985).
[18]R. Blinc, D. C. Ailion, P. Prelovšek, and V. Rutar, Phys. Rev. Lett. **50**, 67 (1983).
[19]R. Blinc, F. Milia, B. Topič, and S. Žumer, Phys. Rev. B **29**, 4173 (1984).
[20]R. Blinc, D. C. Ailion, J. Dolinšek, and S. Žumer, Phys. Rev. Lett. **54**, 79 (1985).